

# SG-Tailor: Inter-Object Commonsense Relationship Reasoning for Scene Graph Manipulation

Haoliang Shang<sup>1,\*</sup> Hanyu Wu<sup>1,\*</sup> Guangyao Zhai<sup>1,2,3</sup> Boyang Sun<sup>1</sup> Fangjinhua Wang<sup>1</sup>  
 Federico Tombari<sup>2,4</sup> Marc Pollefeys<sup>1,5</sup>

<sup>1</sup> ETH Zurich <sup>2</sup> TU Munich <sup>3</sup> MCML <sup>4</sup> Google <sup>5</sup> Microsoft  
 {hshang, hanyuwu}@ethz.ch {guangyao.zhai, federico.tombari}@tum.de  
 {boyang.sun, fangjinhua.wang, marc.pollefeys}@inf.ethz.ch

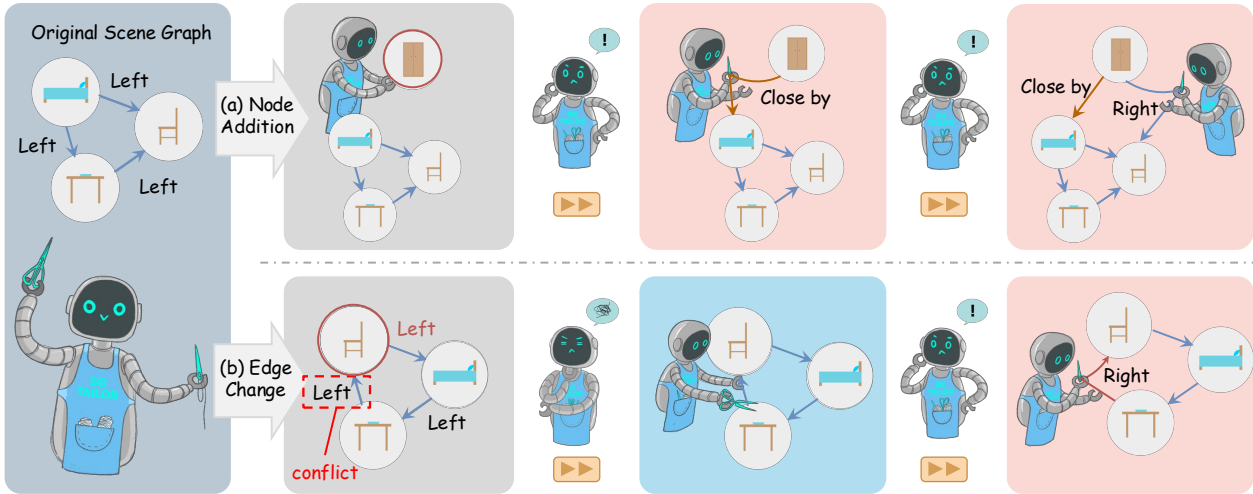


Figure 1. **SG-Tailor for scene graph manipulation.** SG-Tailor manipulates a given scene graph in two modes: (a) *Node Addition* and (b) *Edge Change*. For node addition, SG-Tailor autoregressively **reasons commonsense relationships** between a newly introduced node and existing nodes (e.g., The wardrobe node should be near the bed node and to the left of the chair node, as the chair is already left of the bed.). For edge change, it maintains the desired edge while **resolving conflicts** (e.g., naively moving the chair node to the left of the bed node causes a table conflict. SG-Tailor resolves this by replacing the conflicting edge to maintain coherence).

## Abstract

Scene graphs capture complex relationships among objects, serving as strong priors for content generation and manipulation. Yet, reasonably manipulating scene graphs – whether by adding nodes or modifying edges – remains a challenging and untouched task. Tasks such as adding a node to the graph or reasoning about a node’s relationships with all others are computationally intractable, as even a single edge modification can trigger conflicts due to the intricate interdependencies within the graph. To address these challenges, we introduce SG-Tailor, an autoregressive model that predicts the conflict-free relationship between any two nodes. SG-Tailor not only infers

inter-object relationships, including generating commonsense edges for newly added nodes but also resolves conflicts arising from edge modifications to produce coherent, manipulated graphs for downstream tasks. For node addition, the model queries the target node and other nodes from the graph to predict the appropriate relationships. For edge modification, SG-Tailor employs a Cut-And-Stitch strategy to solve the conflicts and globally adjust the graph. Extensive experiments demonstrate that SG-Tailor outperforms competing methods by a large margin and can be seamlessly integrated as a plug-in module for scene generation and robotic manipulation tasks. The code will be here <sup>1</sup>.

<sup>1</sup><https://github.com/josef5838/SG-Tailor>

## 1. Introduction

Scene graphs effectively capture semantic relationships among objects by representing them as nodes and their interactions as edges [1, 2]. This structured, interpretable representation is widely used in computer vision tasks, such as image captioning [3], scene understanding [4, 5], and robotics applications [6–10].

Additionally, scene graphs uniquely offer a bidirectional capability: they decompose scenes into detailed representations of objects and relationships [11–14], and can compose coherent 2D/3D content based on generative models for advanced applications [14–17]. Building on this foundation, a highly flexible pipeline is envisioned for data creation and manipulation using scene graphs. **First**, a general extractor embeds visual data into scene graphs. **Next**, a graph manipulator modifies these graphs according to user commands, producing diverse yet commonsense-compliant configurations. **Finally**, a generative model synthesizes realistic data from the manipulated graphs for various downstream applications. This streamlined approach significantly enhances flexibility and precision in interactive data generation conditioned on the large amount of 3D scene content [18–20].

While extensive research has addressed the initial graph extraction [21–24] and the final generative synthesis [14, 25–27], scene graph manipulation itself has been largely overlooked. Even though some methods [14, 26, 28] apply manipulation inside their pipeline, they do not consider potential conflicts when changing semantics. However, manipulating scene graphs—whether through node addition or edge modification—is inherently challenging due to their complexity. Even minor changes can cascade through the graph, disrupting overall coherence. For example, adding a node requires not only introducing the new node but also reasoning about its plausible relationships with existing nodes, as shown in Figure 1 (a). Identifying reasonable and commonsense relationships is a complex problem due to the inherent uncertainty and combinatorial complexity of potential relationship combinations. Similarly, modifying a single edge can disturb intricate inter-node dependencies, potentially introducing logical conflicts and making the graph incoherent (see Figure 1 (b) for a case). Identifying and resolving these conflicts to maintain graph consistency remains an unexplored area. Such difficulty steers up when the complexity and scale of the scene graphs increase.

In this work, we propose *SG-Tailor*, an autoregressive model designed to tackle the intricacies of scene graph manipulation. *SG-Tailor* operates by predicting the relationship between any two nodes in the context of an existing scene graph. This capability allows the model to infer commonsense edges for newly added nodes while ensuring that edge modifications do not introduce inconsistencies. Specifically, for node additions, *SG-Tailor* queries the new

node alongside existing nodes to infer their relationships, as depicted in Figure 1 (a). This ensures seamless integration of new nodes into the current scene graph structure. For edge modification, the model employs a novel *Cut-And-Stitch* strategy. First, *SG-Tailor* isolates the subject node from the graph by cutting off all linked edges, then it infers and "stitches" all relationships conditioned on the rest of the graph, thereby removing all possible conflicts in the graph. Through learning, *SG-Tailor* not only learns the spatial constraints but also the inter-object commonsense relationship reasoning to restore global coherence. In such a way, we bypass the computational complexity of detecting and resolving relationship conflicts, particularly in densely connected graphs. We validate *SG-Tailor* through extensive experiments across diverse benchmarks. Results demonstrate that *SG-Tailor* significantly outperforms existing methods and serves as a robust plug-in module for downstream tasks, including scene generation and robotic manipulation. By effectively bridging the gap between theoretical complexity and practical utility, *SG-Tailor* paves new avenues for future research in the manipulation and application of structured visual representations.

Our contributions are summarized as follows:

- We reveal the overlooked problems of scene graph manipulation, highlighting the importance of maintaining semantic coherence during node and edge modifications.
- We propose *SG-Tailor*, an autoregressive model for robust scene graph manipulation capable of commonsense-aware relationship reasoning and conflict solving.
- We demonstrate that *SG-Tailor* not only significantly outperforms existing competitors on diverse benchmarks but also proves its practical effectiveness as a plug-in module for scene generation and robotic manipulation tasks.

## 2. Related work

**Scene Graphs** Scene graphs, as symbolic and semantic representations [3, 23, 29], can be obtained from texts [30], 2D images [12, 31–33], 3D geometry [22, 34] and 4D data [35] for spatial and temporal understanding. Scene graphs can facilitate various tasks, including retrieval [23], generation [14, 25], and VQA [36]. More embodied applications include robotic manipulation [10, 37], and mobile navigation [38]. Most work focuses on how to embed information into the graphs and how to generate concrete content from scene graphs, ignoring the importance of graph manipulation. In this work, we expose this overlooked problem in current work [28] and propose *SG-Tailor* to solve it. The closest work to ours is *SGNet* [39], which predicts objects given the contextual scene graph and the target locations. In contrast, our framework focuses on reasoning inter-object relationships based on textual information without explicit geometric cues.

**Autoregressive Models** Autoregressive models sequentially predict the next component based on previous inputs. In earlier years, It has shown the possibility of generating RGB in a row-by-row, raster-scan manner [40, 41] in image generation. VQGAN [42] further performs autoregressive learning in the latent space of VQVAE [43]. Recently, autoregressive models have dominated natural language processing (NLP), serving as an important component of Multimodal large language models (MLLMs) [44–48]. Beyond text regression, autoregressive models are extended to perform robotics manipulation tasks, serving as a core for vision-language-action models [49–51]. Since scene graphs are natural textual information, we use autoregressive models to treat scene graph manipulation as a next-token prediction task inspired by MLLMs.

### 3. Problem Formulation

We formulate the problem by first defining the set of *Reasonable Scene Graphs* based on scene graph representations. Next, we categorize the operation classes of scene graph manipulation and conduct a comprehensive analysis of the associated challenges, demonstrating that these challenges can be decomposed into *Cut* and *Stitch* steps.

#### 3.1. Reasonable Scene Graph

The scene graph [1] used in this work is denoted by  $G = \{V, E\}$ , which serves as a structured representation of a visual scene.  $V = \{v_i \mid i = 1, \dots, M\}$ , where each  $v_i$  is an object node, and  $E = \{e_{i \rightarrow j} \mid i, j = 1, \dots, M, i \neq j\}$ , where each  $e_{i \rightarrow j}$  is a directed edge from node  $v_i$  to node  $v_j$ . Every node  $v_i$  and edge  $e_{i \rightarrow j}$  incorporate categorical information (class label) about the object and the instance index. Based on  $G$ , we formulate *Reasonable Scene Graphs* as:

$$\mathbb{G} = \{G \in \mathcal{G} \mid G \models P_1 \wedge P_2\}, \quad (1)$$

where  $\mathcal{G}$  denotes the set of all possible scene graphs, and  $P_1, P_2$  denote commonsense constraints and spatial constraints respectively.  $\models$  indicates that the graph  $G$  satisfies these constraints. All reasonable scene graphs have the optimal substructure property, i.e., for any  $G \in \mathbb{G}$ , every subgraph of  $G$  is also reasonable.

#### 3.2. Scene Graph Manipulation

We formally define scene graph manipulation—the process of modifying  $G$  to  $G'$ —as a series of graph-level operations that mirror the adjustments a user might perform on a scene. Although fundamental operations—adding objects, removing objects, and modifying relationships—are conceptually simple, each may result in conflicts and requires precise management, as illustrated in Figure 1. We show that these operations can be reduced to inter-object relationship prediction in an autoregressive fashion.

**Node Addition.** Adding a new object node into the scene graph involves more than a straightforward insertion. To ensure the added node follows the constraints in (1), predominantly the commonsense constraint  $P_1$ , the *Stitch* process requires accurate inter-object reasoning and the establishment of relationships between the new node and all existing nodes. We denote a new node as  $v$ . Define  $\bar{e} \subseteq \{\{v, v_i\} : v_i \in V\}$  as the set of edges between  $v$  and each  $v_i$ . Node addition is then formulated as constructing a new graph

$$G' = (V \cup \{v\}, E \cup \bar{e}) \in \mathbb{G}.$$

Intuitively, every edge in  $\bar{e}$  should not cause conflicts. This can be achieved by sequentially predicting inter-object relationships using an autoregressive approach.

**Node Removal.** Removing a node is a straightforward operation: removing the node and its associated edges, listed as a *Cut* step. Let the node to be removed be  $v \in V$ , and the associated edges are  $\bar{e} \subseteq \{\{v, v_i\} : v_i \in V \setminus \{v\}\}$ , where  $v_i$  are the connected nodes. Thus, it is formulated as constructing a new graph

$$G' = (V \setminus \{v\}, E \setminus \bar{e}) \in \mathbb{G}.$$

**Edge Change.** Modifying spatial relationships is a challenging operation. This task requires case-by-case conflict detection and resolution to ensure compliance with the constraints in (1), particularly the spatial constraints  $P_2$ . This often yields suboptimal results due to heavy engineering requirements and the lack of automatic commonsense reasoning. In contrast, we treat this problem as a *Cut-And-Stitch* process: *Cut*: Temporarily isolate the node of interest by removing its incident edges. *Stitch*: Reinsert the node with its modified relationships and then infer and restore any missing edges, thereby reducing the problem to a node addition task. Let the node of interest be  $v \in V$ . Denote by  $\bar{e}' \subseteq E$  the set of edges originally incident to  $v$  and by  $\bar{e} \subseteq \{\{v, v_i\} : v_i \in V \setminus \{v\}\}$  the set of predicted edges connecting  $v$  to the other nodes. The edge change operation is formulated as constructing a new graph

$$G' = (V, (E \setminus \bar{e}') \cup \bar{e}) \in \mathbb{G}.$$

In summary, by decomposing each operation into a sequence of *Cut* and *Stitch* steps that can be solved by autoregressive inter-object relationship prediction, our formulation systematically addresses the challenges of scene graph manipulation while ensuring that structural coherence is rigorously maintained, i.e.,  $G' \in \mathbb{G}$ .

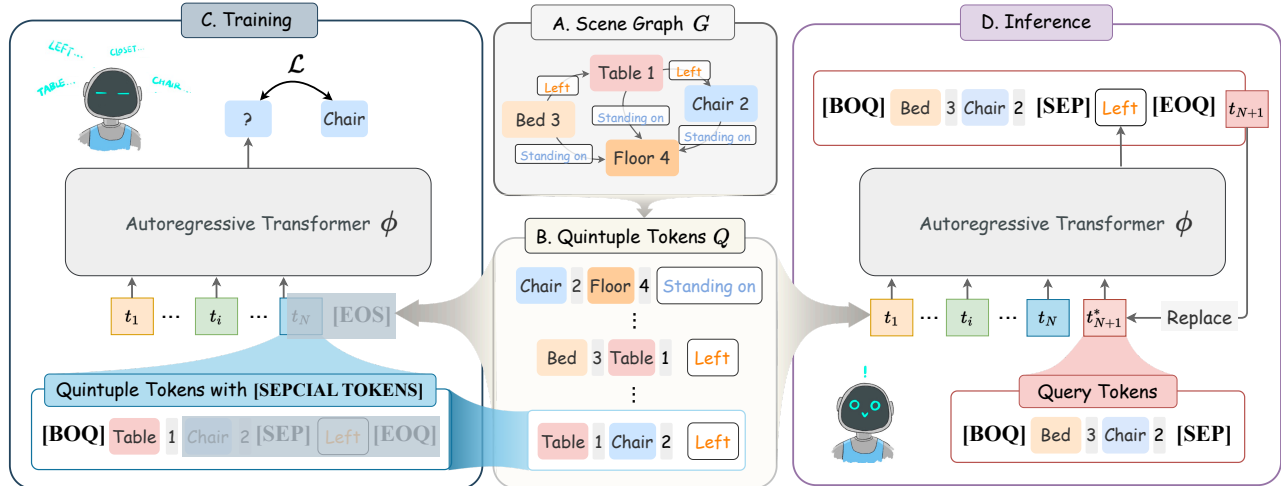


Figure 2. **Training and Inference.** Starting from A. Scene Graph  $G$ , we convert  $N$  triplets into a set of B. Quintuple Tokens  $Q$ , resulting in  $5N$  tokens. Each token  $q_i \in Q$  is then combined with special tokens to form token sequences  $t_i$ . During C. Training, the model  $\phi$  learns to perform next-token prediction, including both object nodes and relationships, with the mask attention mechanism. This process runs until it reaches the sequence-end token [EOS]. During D. Inference,  $\phi$  accepts all existing tokens  $\{t_1, \dots, t_N\}$  from the given graph and query tokens  $t_{N+1}^*$  containing each two of nodes and special tokens to perform next-relationship prediction. The predicted relationship is integrated into  $t_{N+1}^*$ , forming  $t_{N+1}$ . In this way, the model autoregressively reasons about inter-object relationships.

## 4. SG-Tailor

To address the challenges of node addition and edge change (illustrated in Figure 2), we propose SG-Tailor—an autoregressive model that predicts inter-object relationships,  $\bar{e}$ , within a reasonable scene graph. By leveraging a sequential prediction strategy, SG-Tailor infers the appropriate relationships among nodes, ensuring that any newly added node is seamlessly integrated and that the overall graph remains coherent—that is, the manipulated graph  $G' \in \mathbb{G}$ .

### 4.1. From Triplets to Tokens

We formulate inter-object relationship reasoning as an autoregressive sequence generation task by encoding every entity and predicate in the dataset as a unique sequence of tokens. As illustrated in section 3, given a reasonable scene graph  $G \in \mathbb{G}$  with  $|V|$  nodes and  $|E|$  edges, we obtain  $|E|$  triplets, each represented as  $\{v_i, e_{i \rightarrow j}, v_j\}$ . To enable autoregressive modeling based on a Transformer architecture, we first convert these triplets into tokens. Inspired by the quintuple token strategy introduced in [52] for music processing, where each quintuple serves as a unified input to attention blocks, we adopt a similar structure. Specifically, we decompose each triplet into separate tokens representing class labels and instance IDs for the subject and object, along with the predicate, resulting in quintuple tokens:  $q_i = (v_i^{\text{cls}}, v_i^{\text{ind}}, v_j^{\text{cls}}, v_j^{\text{ind}}, e_{i \rightarrow j})$ . We then tokenize each quintuple  $q_i$  into the token sequence  $t_i$  and augment it with special tokens to explicitly guide the learning pro-

cess:

$$t_i = \left( [\text{BOQ}], t_i^1, t_i^2, t_i^3, t_i^4, [\text{SEP}], t_i^p, [\text{EOQ}] \right),$$

where  $t_i^1, t_i^2, t_i^3, t_i^4$  correspond to the tokens for  $v_i^{\text{cls}}, v_i^{\text{ind}}, v_j^{\text{cls}}, v_j^{\text{ind}}$  respectively, and  $t_i^p$  is the predicate token. These special tokens, namely [BOQ], [SEP], [EOQ], clearly delineate the boundaries between subject, object, and relation segments. After the token sequence  $t_N$ , we append a sequence-end token [EOS] (see Figure 2.C).

This tokenization strategy preserves the categorical information, including entity classes and relation types, as well as instance information for each relationship. In other words, the semantic structure of the original scene graph is maintained within the linear token sequence. By encoding triplets as guided token sequences, we enable the model to attend to and learn from the rich structure of the scene graph sequentially.

### 4.2. Next-Token Learning

At the core of SG-Tailor lies a decoder-only transformer  $\phi$  that is trained to generate the scene graph token sequence one token at a time. During training,  $\phi$  is supervised by every token inside of  $t_i$  to learn in diverse domains, including both objects and their relationships. Hence, masking is applied at the individual token level rather than at the level of the entire triplet sequence  $t_i$ , as shown in Figure 2.C. In Sec. 5.5, we demonstrate that it enhances performance by providing diverse supervision rather than solely focusing on the supervision of relationships.



**Modeling** Specifically,  $\phi$  processes input sequences comprising tokens from previous  $\{t_1, t_2, \dots, t_i\}$  and partial tokens  $t_{i+1}^{0:c}$ ,  $0 \leq c < |t_{i+1}|$ , where  $|t_{i+1}|$  denotes the length of the token sequence, to predict the next token  $t_{i+1}^{c+1}$ . Formally, at each prediction step, we have:

$$P(t_{i+1}^{c+1} | t_1, t_2, \dots, t_i, t_{i+1}^{0:c}), \quad \forall i \leq N - 1, \quad (2)$$

This autoregressive modeling enables  $\phi$  to capture intricate dependencies at both the entity level and relationship level across the entire sequence, thus enhancing the reasoning capability on inter-object relationships.

**Training Objective** We adopt a categorical cross-entropy loss across the entire vocabulary to train the model:

$$\mathcal{L} = - \sum_{t=1}^T \log \frac{\exp(z_{t,y_t})}{\sum_{w \in \mathcal{V}} \exp(z_{t,w})}, \quad (3)$$

where  $T$  is the total number of tokens in the sequence,  $\mathcal{V}$  represents the token vocabulary,  $y_t$  denotes the ground-truth token at step  $t$ , and  $z_{t,w}$  indicates the logit (unnormalized score) assigned by the model to token  $w$  at step  $t$ . This loss guides the model to accurately predict each token, ensuring the effective autoregressive modeling of scene graph structures.

### 4.3. Next-Relationship Reasoning

During inference, SG-Tailor performs autoregressive reasoning to predict the inter-object relationship between a query node and another node, conditioning each prediction on the previously established graph connections. Given contextual token sequences  $T = \{t_i | i = 1, \dots, N\}$  representing the existing graph, the model computes the conditional probability on the query tokens consisting of the query node and the other nodes to have

$$t_{i+1}^* = ([\mathbf{BOQ}], t_i^1, t_i^2, t_i^3, t_i^4, [\mathbf{SEP}]). \quad (4)$$

Then, the reasoning can be formulated as  $P(t_i^p | T, t_{i+1}^*)$ . This formulation enables the model to capture the intricate interdependencies among objects, ensuring that each new prediction respects the existing graph structure.

During every inference step, the subject and object tokens are queried as described in Figure 2.D, and the model predicts the next possible token using a top- $p$  (nucleus) sampling strategy [53], in which the probability distribution is first sorted in descending order, and then only the smallest set of tokens whose cumulative probability exceeds a predefined threshold  $p = 0.7$  is considered for sampling. By the end of the inference, the scene graph  $G' \in \mathbb{G}$  is built from the tokens.

## 5. Experiments

### 5.1. Datasets

We evaluate our method quantitatively and qualitatively on four datasets, 3RScan [54], 3D-FRONT [55], SG-Bot [37], and SceneVerse [18] with different motivations. Both 3RScan and 3D-FRONT are widely used as benchmarks for scene-graph-based 3D scene generation [26, 28], which allows qualitative evaluation of our method on the 3D scene generation downstream task. Experiments on SceneVerse37K, a subset of the complete SceneVerse dataset, show the scalability of our method in large-scale scenarios.

Due to the absence of source-target 3D scene pairs in 3RScan and 3D-FRONT, we evaluate the user preference ranking of our method compared to a baseline based on SceneGraphNet [39], the naive manipulation baseline described in [28], and the response from an instruction fine-tuned large language model Llama-3.3-70B-Instruct [56]. In addition to scene manipulation, we train our method on the SG-Bot dataset [37] to evaluate how our method facilitates scene-graph-based robotic manipulation.

Training data is generated by encoding scene graph labels into sequences of tokens from our vocabulary.

### 5.2. Implementation Details

We use Llama [44] layers as the autoregressive transformer in our model, with a hidden size of 688 and 12 attention heads. We pad the scene graph sequence to the context length 1024 and use a cosine learning rate scheduler with an initial learning rate of  $5 \times 10^{-4}$  and a weight decay of  $1 \times 10^{-2}$ . The batch size is set to 16 in all our experiments, and we train our models for 50 epochs, employing early stopping. Unless otherwise specified, we predict all relationships using nucleus sampling [53] with a p-value of 0.7. We augment our data by randomly shuffling each scene graph three times.

### 5.3. Baselines

**Naive Manipulation Baseline (Naive).** Following [15, 26], we propose a baseline based on [28]. It simply modifies a target edge without any manipulation of the rest of the graph. Since this baseline cannot reason relationships, we remove it from node addition tasks.

**SceneGraphNet (SGNet).** SceneGraphNet is a Message-Passing Neural Network inspired by GNN [39]. We modify SGNet as a baseline. Since SGNet uses class labels, location, and dimension information to predict the likelihood over classes at a query location, we modify the encoder part to only process class information, keep the message-passing mechanism, and build two MLP decoders for our tasks of node addition and edge change, respectively.

**LLM (Llama-3.3).** We use the latest Llama model, the

Llama-3.3-70B-Instruct [56], as our baseline. Specifically, we prompt the model with the task description, all the triplets describing a given scene, and the specific relationship we aim to modify. The LLM then processes this information and generates a revised scene graph based on our prompt. A detailed prompt template used for the edge change task on the dataset 3D-FRONT can be found in the supplementary.

## 5.4. Evaluation Metrics

We evaluate our method with two types of quantitative metrics: the ranking-based metrics and the scene graph consistency metrics.

**Ranking-based Evaluation Metrics.** Since the accuracy of a predicted edge depends on scene context and multiple valid answers may exist, we adopt ranking-based metrics from the knowledge graph community [57]. Please refer to the supplementary for the equations for these metrics.

**Mean Rank (MR)** calculates the average ranking position of correct predictions, where lower ranks indicate better performance; outliers can skew results.

**Mean Reciprocal Rank (MRR)** averages the reciprocal rank of the first correct prediction, emphasizing early correct answers and penalizing lower-ranked, delayed correct predictions.

**Hit@K** computes the proportion of queries where the correct answer appears within the top K predictions, reflecting practical recommendation performance.

**Scene Graph Consistency Metric.** Taking the intuition that the presence of a cycle signifies a spatial contradiction within the scene graph, we identify spatial conflicts through Algorithm 1 in supplementary material, a simple graph loop detection algorithm based on depth-first search. We convert left and behind triplets into their right and front counterparts and then detect cycles in the right and front relationships. This experiment is conducted among the naive approach, Llama-3.3-70B-Instruct, SceneGraphNet, and our approach by modifying spatial relations (left, right, front, behind) to generate new scene graphs.

## 5.5. Ablation Study

We also evaluate our method against two other variants based on the same dataset and evaluation metrics in Table 1. Specifically, we test the following variants: (1) **SG-Tailor (GPT-2)**. We train the GPT-2 layers [58] of the same depth and width on the same next token prediction task. (2) **SG-Tailor (Next-Rel)** We train SG-tailor with loss label masks on all subjects and objects, effectively guiding the model to only learn to predict the predicates. We found that our method outperforms all these variants.

## 5.6. Quantitative Results

We compare the performance of our method to the baseline method on several different datasets.

**Performance on 3RScan:** On the 3RScan dataset, our method achieves notable improvements over SGNet. Specifically, our approach reduces the MR from 3.9872 to 3.7636, indicating a more accurate ranking of true relationships. Furthermore, our method boosts the MRR from 0.5719 to 0.6241 and the Hit@1 score from 0.3974 to 0.4511. These enhancements suggest that our method is significantly better at prioritizing correct relationships in the ranking process.

**Performance on SceneVerse:** Our full SG-Tailor model performs better than the baseline on this large-scale and challenging dataset on all metrics with a **5.52%** relative increase on Hit@1. We argue that SGNet is based on GRU and has less generalization ability.

**Performance on 3D-FRONT:** On the 3D-FRONT dataset, our final configuration delivers an **11.9%** reduction in MR (from 4.1029 to 3.6129) and achieves superior Hit@1 (0.3048 vs. 0.2708) and Hit@10 (0.9833 vs. 0.9433) scores compared to SGNet. While the overall MRR and Hit@3 scores remain competitive, our GPT-2 variant further excels on Hit@3 (0.6121), highlighting the potential benefits of incorporating language model features for specific ranking aspects.

**Scene Graph Consistency Result:** In addition to ranking metrics, we evaluate the cycle rate of the manipulated scene graphs, as shown in Table 2. Notably, over 30% of the scene graphs generated by the naive approach contain significant contradictions, whereas our method effectively mitigates these inconsistencies, achieving a remarkably low cycle rate of just 1%. We infer that the exceptionally high cycle rate observed for the LLM is likely due to the fact that instruction-tuned LLMs are prone to noise[59]. Overall, these quantitative results clearly demonstrate that conditioning on the entire scene graph context not only improves the ranking accuracy of relationship predictions but also yields more coherent and spatially consistent scene graphs. The consistent performance gains across different datasets and metrics underscore the robustness and effectiveness of our approach.

## 6. Downstream Applications

### 6.1. Scene Manipulation

In this section, we evaluate our method on the downstream task of scene manipulation. Operating entirely at the scene graph level, our model integrates seamlessly with existing scene-graph-based 3D scene generation frameworks [15, 26, 28]. We train SG-Tailor on the 3D-FRONT dataset—the same dataset used for the downstream module Graph-to-3D—and perform scene graph manipulation before feed-

Method	Dataset	MR ↓	MRR ↑	Hit@1 ↑	Hit@3 ↑	Hit@10 ↑
SGNet [39]	3RScan [54]	3.987	0.572	0.398	<b>0.683</b>	0.941
Ours		<b>3.764</b>	<b>0.624</b>	<b>0.451</b>	0.681	<b>0.953</b>
SGNet [39]	SceneVerse37K [18]	5.922	0.367	0.199	0.426	0.882
Ours		<b>5.623</b>	<b>0.374</b>	<b>0.210</b>	<b>0.507</b>	<b>0.92</b>
SGNet [39]	3D-FRONT [55]	4.103	0.486	0.271	0.593	0.943
Ours (GPT-2)		4.113	0.472	0.273	<b>0.604</b>	0.947
Ours (Next-Rel)		4.113	0.476	0.282	0.603	0.951
Ours		<b>3.613</b>	<b>0.498</b>	<b>0.305</b>	0.591	<b>0.983</b>

Table 1. Performance metrics across models and datasets. Best results are in bold

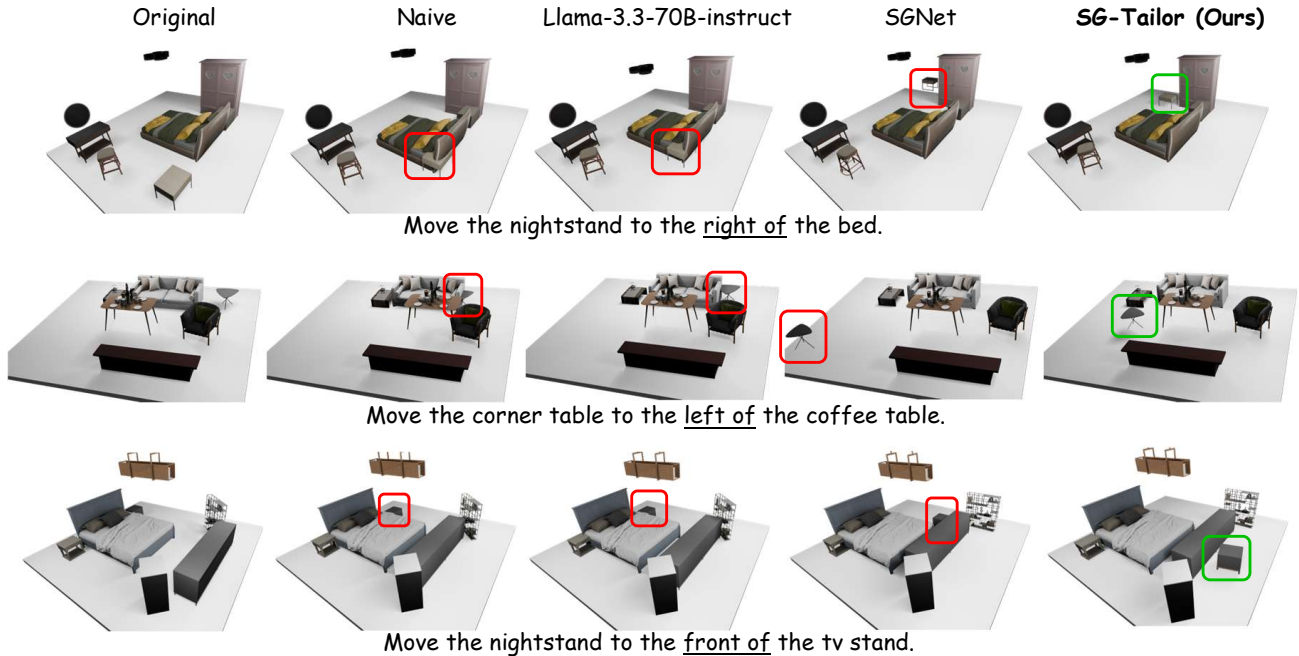


Figure 3. **Qualitative comparison.** We assess the quality of scene graph manipulation across different methods by generating the corresponding scenes using the Graph-to-3D model. [28].

Method	right cycle ↓	front cycle ↓	total ↓
Naive	19.19%	19.73%	38.92%
Llama-3.3 [56]	34.48%	31.03%	62.07%
SGNet [39]	7.37%	<b>0.0</b>	7.37%
SG-Tailor (Ours)	<b>1.05%</b>	<b>0.0</b>	<b>1.05%</b>

Table 2. **Cycle rate.** The percentage of scene graphs that have either a right or front cycle. The best results are in bold.

Method	manipulation ↑	addition ↑
Naive	1.72%	-
Llama-3.3 [56]	9.48%	18.97%
SGNet [39]	18.10%	33.33%
SG-Tailor (Ours)	<b>70.69%</b>	<b>47.70%</b>

Table 3. **Top-1 rate.** The percentage of participants who consider each method across different tasks. The best results are in bold.

ing the graph into Graph-to-3D for 3D rendering. We compare the rendered results of our method with those of SGNet, LLM, and a naive edge-change approach implemented in Graph-to-3D. Additionally, we conduct a percep-

tual study to gauge user preferences: the study evaluates four methods on the edge-change task and, for the node addition task, excludes the naive method, which lacks the spatial inference ability to integrate a new node into the scene.

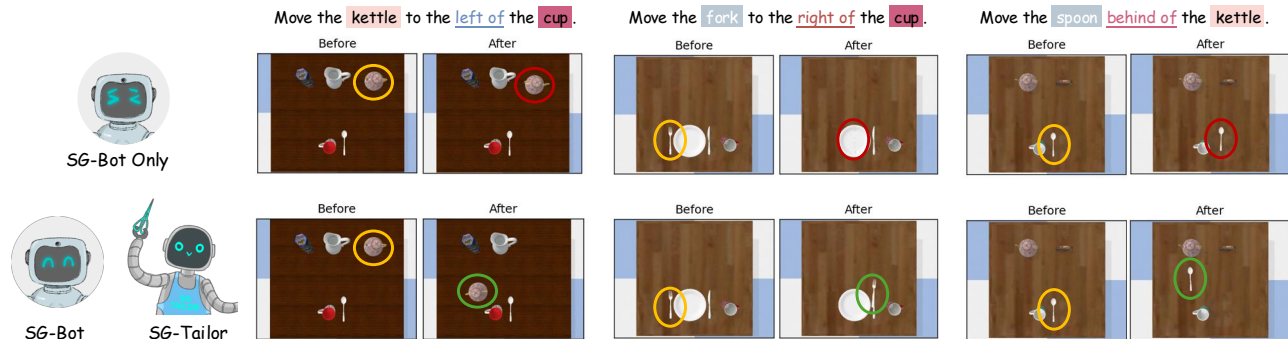


Figure 4. **Qualitative comparison of SG-Bot w/ and w/o SG-Tailor.** We show three examples of SG-Tailor facilitating the robotic manipulation tasks. More examples can be found in the supplementary.

**Qualitative Results.** Our scene graph manipulation method demonstrates strong potential for enhancing 3D scene generation. By modifying the relationships within a scene graph, our approach can generate a diverse range of 3D scenes. To assess the quality of the manipulated graphs, we render the corresponding 3D scenes using Graph-to-3D (see Figure 3). Our method effectively captures the global context, resulting in scene graphs that are both accurate and coherent. In contrast, alternative methods struggle to enforce object constraints and predict new relationships accurately, often leading to inconsistent object placements and unrealistic arrangements in the scenes.

**User Study.** To compensate for the lack of ground-truth 3D scenes after manipulation, we conducted a perceptual evaluation study with 30 randomly selected participants. In the edge change part, participants are presented with the original scene and scenes generated by four different methods: naive, SNet, LLM, and SG-Tailor. In the node addition part only results from LLM, SNet, and SG-Tailor are compared. Participants rank the scenes according to how well the changes in the scenes reflect the perceptual similarity to the provided task description. The summarized results in Table 3 demonstrate that our method outperforms all others in both node addition and edge change tasks.

## 6.2. Robotic Manipulation

Beyond scene manipulation, we integrate SG-Tailor into robotic manipulation tasks within tabletop environments. Our approach builds upon SG-Bot [37], a robotic manipulation method that leverages graph generative models to determine goal states. While SG-Bot excels at generating precise target configurations, it often encounters difficulties rearranging objects when conflicts emerge in the scene graph following relationship updates. As illustrated in Figure 4, SG-Tailor overcomes these challenges by employing our novel *Cut-And-Stitch* strategy combined with robust inter-object reasoning. This integration produces more coherent

and context-aware scene representations, significantly enhancing SG-Bot’s planning accuracy and execution efficiency. Additional qualitative results, including a detailed image stream, are presented in the Supplementary.

## 7. Limitation

We observed that our SG-Tailor model does not perform well when the training scene graphs are overly noisy. For example, an excessive number of non-spatial relationships, such as *same material as*, can confuse the model, leading it to prioritize predicting these relationships rather than focusing on spatial constraints. Another potential area for improvement lies in our current approach to manipulating objects within the scene graph. When modifying an object, we remove all edges connected to its node and predict new edges. However, this approach may be simplistic and brute-force, as it disregards contextual information from the original connections, potentially leading to undesired scene graph modifications.

## 8. Conclusion

We present SG-Tailor, an autoregressive model for scene graph manipulation that addresses the limitations of existing methods by considering the global scene context and commonsense relationships. Unlike prior approaches that modify individual edges in isolation, our model predicts new relationships conditioned on the entire scene graph, ensuring spatial consistency. Experimental results demonstrate that SG-Tailor generates more realistic and contradiction-free 3D scenes. This work opens new directions for intelligent and context-aware scene generation, with potential applications in areas such as diverse 3D scene generation and robotics manipulation.



## References

- [1] Hongsheng Li, Guangming Zhu, Liang Zhang, Youliang Jiang, Yixuan Dang, Haoran Hou, Peiyi Shen, Xia Zhao, Syed Afaq Ali Shah, and Mohammed Bennamoun. Scene graph generation: A comprehensive survey. *Neurocomputing*, 566:127052, 2024. 2, 3
- [2] Xiaojun Chang, Pengzhen Ren, Pengfei Xu, Zhihui Li, Xiaojiang Chen, and Alex Hauptmann. A comprehensive survey of scene graphs: Generation and application. *IEEE Transactions on Pattern Analysis and Machine Intelligence*, 45(1): 1–26, 2021. 2
- [3] Ranjay Krishna, Yuke Zhu, Oliver Groth, Justin Johnson, Kenji Hata, Joshua Kravitz, Stephanie Chen, Yannis Kalantidis, Li-Jia Li, David A Shamma, et al. Visual genome: Connecting language and vision using crowdsourced dense image annotations. *International journal of computer vision*, 123:32–73, 2017. 2
- [4] Cheng Zhang, Zhaopeng Cui, Yinda Zhang, Bing Zeng, Marc Pollefeys, and Shuaicheng Liu. Holistic 3d scene understanding from a single image with implicit representation. In *Proceedings of the IEEE/CVF Conference on Computer Vision and Pattern Recognition*, pages 8833–8842, 2021. 2
- [5] Qiao Gu, Ali Kuwajerwala, Sacha Morin, Krishna Murthy Jatavallabhula, Bipasha Sen, Aditya Agarwal, Corban Rivera, William Paul, Kirsty Ellis, Rama Chellappa, et al. Conceptgraphs: Open-vocabulary 3d scene graphs for perception and planning. In *2024 IEEE International Conference on Robotics and Automation (ICRA)*, pages 5021–5028. IEEE, 2024. 2
- [6] Yun Chang, Nathan Hughes, Aaron Ray, and Luca Carlone. Hydra-multi: Collaborative online construction of 3d scene graphs with multi-robot teams. In *2023 IEEE/RSJ International Conference on Intelligent Robots and Systems (IROS)*, pages 10995–11002. IEEE, 2023. 2
- [7] Nathan Hughes, Yun Chang, and Luca Carlone. Hydra: A real-time spatial perception system for 3d scene graph construction and optimization. *arXiv preprint arXiv:2201.13360*, 2022.
- [8] Abdelrhman Werby, Chenguang Huang, Martin Büchner, Abhinav Valada, and Wolfram Burgard. Hierarchical open-vocabulary 3d scene graphs for language-grounded robot navigation. In *First Workshop on Vision-Language Models for Navigation and Manipulation at ICRA 2024*, 2024.
- [9] Dominic Maggio, Yun Chang, Nathan Hughes, Matthew Trang, Dan Griffith, Carlyn Dougherty, Eric Cristofalo, Lukas Schmid, and Luca Carlone. Clio: Real-time task-driven open-set 3d scene graphs. *IEEE Robotics and Automation Letters*, 2024.
- [10] Hanxiao Jiang, Binghao Huang, Ruihai Wu, Zhuoran Li, Shubham Garg, Hooshang Nayyeri, Shenlong Wang, and Yunzhu Li. Roboexp: Action-conditioned scene graph via interactive exploration for robotic manipulation. *arXiv preprint arXiv:2402.15487*, 2024. 2
- [11] Jianwei Yang, Jiasen Lu, Stefan Lee, Dhruv Batra, and Devi Parikh. Graph r-cnn for scene graph generation. In *Proceedings of the European conference on computer vision (ECCV)*, pages 670–685, 2018. 2
- [12] Danfei Xu, Yuke Zhu, Christopher B Choy, and Li Fei-Fei. Scene graph generation by iterative message passing. In *Proceedings of the IEEE conference on computer vision and pattern recognition*, pages 5410–5419, 2017. 2
- [13] Kaihua Tang, Yulei Niu, Jianqiang Huang, Jiaxin Shi, and Hanwang Zhang. Unbiased scene graph generation from biased training. In *Proceedings of the IEEE/CVF conference on computer vision and pattern recognition*, pages 3716–3725, 2020.
- [14] Helisa Dharmo, Azade Farshad, Iro Laina, Nassir Navab, Gregory D Hager, Federico Tombari, and Christian Rupprecht. Semantic image manipulation using scene graphs. In *Proceedings of the IEEE/CVF conference on computer vision and pattern recognition*, pages 5213–5222, 2020. 2
- [15] Guangyao Zhai, Evin Pinar Örnek, Dave Zhenyu Chen, Ruotong Liao, Yan Di, Nassir Navab, Federico Tombari, and Benjamin Busam. Echoscene: Indoor scene generation via information echo over scene graph diffusion. In *European Conference on Computer Vision*, pages 167–184. Springer, 2024. 5, 6
- [16] Chenguo Lin and Yadong Mu. Instructscene: Instruction-driven 3d indoor scene synthesis with semantic graph prior. *arXiv preprint arXiv:2402.04717*, 2024.
- [17] Gege Gao, Weiyang Liu, Anpei Chen, Andreas Geiger, and Bernhard Schölkopf. Graphdreamer: Compositional 3d scene synthesis from scene graphs. In *Proceedings of the IEEE/CVF Conference on Computer Vision and Pattern Recognition*, pages 21295–21304, 2024. 2
- [18] Baoxiong Jia, Yixin Chen, Huangyue Yu, Yan Wang, Xuesong Niu, Tengyu Liu, Qing Li, and Siyuan Huang. Sceneverse: Scaling 3d vision-language learning for grounded scene understanding. In *European Conference on Computer Vision (ECCV)*, 2024. 2, 5, 7
- [19] Johanna Wald, Helisa Dharmo, Nassir Navab, and Federico Tombari. Learning 3d semantic scene graphs from 3d indoor reconstructions. In *Proceedings of the IEEE/CVF Conference on Computer Vision and Pattern Recognition*, pages 3961–3970, 2020.
- [20] Santhosh Kumar Ramakrishnan, Aaron Gokaslan, Erik Wijmans, Oleksandr Maksymets, Alexander Clegg, John M Turner, Eric Undersander, Wojciech Galuba, Andrew Westbury, Angel X Chang, Manolis Savva, Yili Zhao, and Dhruv Batra. Habitat-matterport 3d dataset (HM3d): 1000 large-scale 3d environments for embodied AI. In *Thirty-fifth Conference on Neural Information Processing Systems Datasets and Benchmarks Track*, 2021. URL <https://arxiv.org/abs/2109.08238>. 2
- [21] Shun-Cheng Wu, Johanna Wald, Keisuke Tateno, Nassir Navab, and Federico Tombari. Scenegraphfusion: Incremental 3d scene graph prediction from rgb-d sequences. In *Proceedings of the IEEE/CVF Conference on Computer Vision and Pattern Recognition*, pages 7515–7525, 2021. 2
- [22] Antoni Rosinol, Andrew Violette, Marcus Abate, Nathan Hughes, Yun Chang, Jingnan Shi, Arjun Gupta, and Luca Carlone. Kimera: From slam to spatial perception with 3d dynamic scene graphs. *The International Journal of Robotics Research*, 40(12-14):1510–1546, 2021. 2

- [23] Justin Johnson, Ranjay Krishna, Michael Stark, Li-Jia Li, David Shamma, Michael Bernstein, and Li Fei-Fei. Image retrieval using scene graphs. In *Proceedings of the IEEE conference on computer vision and pattern recognition*, pages 3668–3678, 2015. 2
- [24] Jinbae Im, JeongYeon Nam, Nokyung Park, Hyungmin Lee, and Seunghyun Park. Egtr: Extracting graph from transformer for scene graph generation. In *Proceedings of the IEEE/CVF Conference on Computer Vision and Pattern Recognition*, pages 24229–24238, 2024. 2
- [25] Justin Johnson, Agrim Gupta, and Li Fei-Fei. Image generation from scene graphs. In *Proceedings of the IEEE conference on computer vision and pattern recognition*, pages 1219–1228, 2018. 2
- [26] Guangyao Zhai, Evin Pınar Örneke, Shun-Cheng Wu, Yan Di, Federico Tombari, Nassir Navab, and Benjamin Busam. Commonsences: Generating commonsense 3d indoor scenes with scene graph diffusion. In *Thirty-seventh Conference on Neural Information Processing Systems*, 2023. URL <https://openreview.net/forum?id=1SF2tiopYJ>. 2, 5, 6
- [27] Zhifei Yang, Keyang Lu, Chao Zhang, Jiaying Qi, Hanqi Jiang, Ruifei Ma, Shenglin Yin, Yifan Xu, Mingzhe Xing, Zhen Xiao, et al. Mmgdreamer: Mixed-modality graph for geometry-controllable 3d indoor scene generation. *arXiv preprint arXiv:2502.05874*, 2025. 2
- [28] Helisa Dhama, Fabian Manhardt, Nassir Navab, and Federico Tombari. Graph-to-3d: End-to-end generation and manipulation of 3d scenes using scene graphs. In *Proceedings of the IEEE/CVF International Conference on Computer Vision*, pages 16352–16361, 2021. 2, 5, 6, 7
- [29] Iro Armeni, Zhi-Yang He, JunYoung Gwak, Amir R Zamir, Martin Fischer, Jitendra Malik, and Silvio Savarese. 3d scene graph: A structure for unified semantics, 3d space, and camera. In *Proceedings of the IEEE/CVF international conference on computer vision*, pages 5664–5673, 2019. 2
- [30] Chengyang Zhao, Yikang Shen, Zhenfang Chen, Mingyu Ding, and Chuang Gan. Textpsg: Panoptic scene graph generation from textual descriptions. In *Proceedings of the IEEE/CVF International Conference on Computer Vision*, pages 2839–2850, 2023. 2
- [31] Rowan Zellers, Mark Yatskar, Sam Thomson, and Yejin Choi. Neural motifs: Scene graph parsing with global context. In *Proceedings of the IEEE conference on computer vision and pattern recognition*, pages 5831–5840, 2018. 2
- [32] Mengshi Qi, Weijian Li, Zhengyuan Yang, Yunhong Wang, and Jiebo Luo. Attentive relational networks for mapping images to scene graphs. In *Proceedings of the IEEE/CVF Conference on Computer Vision and Pattern Recognition*, pages 3957–3966, 2019.
- [33] Roei Herzig, Moshiko Raboh, Gal Chechik, Jonathan Berant, and Amir Globerson. Mapping images to scene graphs with permutation-invariant structured prediction. *Advances in Neural Information Processing Systems*, 31, 2018. 2
- [34] Sebastian Koch, Pedro Hermosilla, Narunas Vaskevicius, Mirco Colosi, and Timo Ropinski. Sgrec3d: Self-supervised 3d scene graph learning via object-level scene reconstruction. In *Proceedings of the IEEE/CVF Winter Conference on Applications of Computer Vision*, pages 3404–3414, 2024. 2
- [35] Jingkang Yang, Jun Cen, Wenxuan Peng, Shuai Liu, Fangzhou Hong, Xiangtai Li, Kaiyang Zhou, Qifeng Chen, and Ziwei Liu. 4d panoptic scene graph generation. *Advances in Neural Information Processing Systems*, 36: 69692–69705, 2023. 2
- [36] Damien Teney, Lingqiao Liu, and Anton van Den Hengel. Graph-structured representations for visual question answering. In *Proceedings of the IEEE conference on computer vision and pattern recognition*, pages 1–9, 2017. 2
- [37] Guangyao Zhai, Xiaoni Cai, Dianye Huang, Yan Di, Fabian Manhardt, Federico Tombari, Nassir Navab, and Benjamin Busam. Sg-bot: Object rearrangement via coarse-to-fine robotic imagination on scene graphs. In *2024 IEEE International Conference on Robotics and Automation (ICRA)*, pages 4303–4310. IEEE, 2024. 2, 5, 8
- [38] Krishan Rana, Jesse Haviland, Sourav Garg, Jad Abou-Chakra, Ian Reid, and Niko Suenderhauf. Sayplan: Grounding large language models using 3d scene graphs for scalable robot task planning. *arXiv preprint arXiv:2307.06135*, 2023. 2
- [39] Yang Zhou, Zachary While, and Evangelos Kalogerakis. Scenegraphnet: Neural message passing for 3d indoor scene augmentation. In *IEEE Conference on Computer Vision (ICCV)*, 2019. 2, 5, 7
- [40] Aaron Van den Oord, Nal Kalchbrenner, Lasse Espeholt, Oriol Vinyals, Alex Graves, et al. Conditional image generation with pixelcnn decoders. *Advances in neural information processing systems*, 29, 2016. 3
- [41] Mark Chen, Alec Radford, Rewon Child, Jeffrey Wu, Heewoo Jun, David Luan, and Ilya Sutskever. Generative pre-training from pixels. In *International conference on machine learning*, pages 1691–1703. PMLR, 2020. 3
- [42] Patrick Esser, Robin Rombach, and Bjorn Ommer. Taming transformers for high-resolution image synthesis. In *Proceedings of the IEEE/CVF conference on computer vision and pattern recognition*, pages 12873–12883, 2021. 3
- [43] Aaron Van Den Oord, Oriol Vinyals, et al. Neural discrete representation learning. *Advances in neural information processing systems*, 30, 2017. 3
- [44] Hugo Touvron, Thibaut Lavril, Gautier Izacard, Xavier Martinet, Marie-Anne Lachaux, Timothée Lacroix, Baptiste Rozière, Naman Goyal, Eric Hambro, Faisal Azhar, Aurelien Rodriguez, Armand Joulin, Edouard Grave, and Guillaume Lample. Llama: Open and efficient foundation language models, 2023. URL <https://arxiv.org/abs/2302.13971>. 3, 5
- [45] Tom Brown, Benjamin Mann, Nick Ryder, Melanie Subbiah, Jared D Kaplan, Prafulla Dhariwal, Arvind Neelakantan, Pranav Shyam, Girish Sastry, Amanda Askell, et al. Language models are few-shot learners. *Advances in neural information processing systems*, 33:1877–1901, 2020.
- [46] Jean-Baptiste Alayrac, Jeff Donahue, Pauline Luc, Antoine Miech, Iain Barr, Yana Hasson, Karel Lenc, Arthur Mensch, Katherine Millican, Malcolm Reynolds, et al. Flamingo: a visual language model for few-shot learning. *Advances*

- in neural information processing systems*, 35:23716–23736, 2022.
- [47] Daya Guo, Dejian Yang, Haowei Zhang, Junxiao Song, Ruoyu Zhang, Runxin Xu, Qihao Zhu, Shirong Ma, Peiyi Wang, Xiao Bi, et al. Deepseek-r1: Incentivizing reasoning capability in llms via reinforcement learning. *arXiv preprint arXiv:2501.12948*, 2025.
- [48] Haotian Liu, Chunyuan Li, Qingyang Wu, and Yong Jae Lee. Visual instruction tuning. *Advances in neural information processing systems*, 36:34892–34916, 2023. 3
- [49] Octo Model Team, Dibya Ghosh, Homer Walke, Karl Pertsch, Kevin Black, Oier Mees, Sudeep Dasari, Joey Hejna, Tobias Kreiman, Charles Xu, et al. Octo: An open-source generalist robot policy. *arXiv preprint arXiv:2405.12213*, 2024. 3
- [50] Moo Jin Kim, Karl Pertsch, Siddharth Karamcheti, Ted Xiao, Ashwin Balakrishna, Suraj Nair, Rafael Rafailov, Ethan Foster, Grace Lam, Pannag Sanketi, et al. Openvla: An open-source vision-language-action model. *arXiv preprint arXiv:2406.09246*, 2024.
- [51] Kevin Black, Noah Brown, Danny Driess, Adnan Esmail, Michael Equi, Chelsea Finn, Niccolo Fusai, Lachy Groom, Karol Hausman, Brian Ichter, et al. A vision-language-action flow model for general robot control. *arXiv preprint arXiv:2410.24164*, 2024. 3
- [52] Jinlong Zhu, Keigo Sakurai, Ren Togo, Takahiro Ogawa, and Miki Haseyama. Mmt-bert: Chord-aware symbolic music generation based on multitrack music transformer and musicbert. *arXiv preprint arXiv:2409.00919*, 2024. 4
- [53] Ari Holtzman, Jan Buys, Li Du, Maxwell Forbes, and Yejin Choi. The curious case of neural text degeneration, 2020. URL <https://arxiv.org/abs/1904.09751>. 5
- [54] Johanna Wald, Armen Avetisyan, Nassir Navab, Federico Tombari, and Matthias Niessner. Rio: 3d object instance re-localization in changing indoor environments. In *Proceedings IEEE International Conference on Computer Vision (ICCV)*, 2019. 5, 7
- [55] Huan Fu, Bowen Cai, Lin Gao, Lingxiao Zhang, Jiaming Wang, Cao Li, Zengqi Xun, Chengyue Sun, Rongfei Jia, Binqiang Zhao, and Hao Zhang. 3d-front: 3d furnished rooms with layouts and semantics, 2021. URL <https://arxiv.org/abs/2011.09127>. 5, 7
- [56] Aaron Grattafiori, Abhimanyu Dubey, Abhinav Jauhri, Abhinav Pandey, Abhishek Kadian, Ahmad Al-Dahle, Aiesha Letman, Akhil Mathur, Alan Schelten, Alex Vaughan, et al. The llama 3 herd of models. *arXiv preprint arXiv:2407.21783*, 2024. 5, 6, 7, 12
- [57] Antoine Bordes, Nicolas Usunier, A. Garcia-Duran, Jason Weston, and Oksana Yakhnenko. Translating embeddings for modeling multi-relational data. In *Neural Information Processing Systems*, 2013. 6
- [58] Alec Radford, Jeff Wu, Rewon Child, David Luan, Dario Amodei, and Ilya Sutskever. Language models are unsupervised multitask learners. 2019. 6
- [59] Taehyeon Kim, Joonkeek Kim, Gihun Lee, and Se-Young Yun. Instructive decoding: Instruction-tuned large language models are self-refiner from noisy instructions, 2024. URL <https://arxiv.org/abs/2311.00233>. 6

## Supplementary Materials

### A. Metrics

As discussed in the main paper, we evaluate our method with ranking-based metrics: mean rank, mean reciprocal rank, and Hits@k. The detailed definition is as follows:

#### Mean Rank (MR)

$$\text{MR} = \frac{1}{N} \sum_{i=1}^N \text{rank}_i. \quad (5)$$

#### Mean Reciprocal Rank (MRR)

$$\text{MRR} = \frac{1}{N} \sum_{i=1}^N \frac{1}{\text{rank}_i}. \quad (6)$$

#### Hit@k

$$\text{Hit@k} = \frac{1}{N} \sum_{i=1}^N \mathbb{1}\{\text{rank}_i \leq k\}. \quad (7)$$

### B. Cycle Detect Algorithm

We identify spatial conflicts through Algorithm 1, which is a graph loop detection algorithm based on depth-first search (DFS). Specifically, we convert left and behind triplets into their right and front counterparts and then detect cycles in the right and front relationships.

---

**Algorithm 1** DFS-based Cycle Detection in a Directed Graph

---

```
1: procedure DETECTCYCLE( $G$ )
2:    $visited \leftarrow \emptyset$ 
3:    $recStack \leftarrow \emptyset$ 
4:   for each vertex  $v$  in  $G$  do
5:     if  $v \notin visited$  then
6:       if DFS( $v, visited, recStack, G$ ) then
7:         return true           ▷ Cycle detected
8:       end if
9:     end if
10:  end for
11:  return false             ▷ No cycle found
12: end procedure
```

---

### C. LLM Manipulation Prompt

We provide the prompts that we use for the edge change task with Llama-3.3-70B-Instruct [56].

[Context]  
You are a helpful assistant whose task is to manipulate a node in a scene graph. The scene graph is represented as triplets in the following format:

subject object relationship

Possible relationships are:

left  
right  
front  
behind  
standing\_on  
bigger\_than  
smaller\_than

Input Format:

First line: The triplet of the node to be set.

Subsequent lines: Existing scene graph triplets (one per line).

Instructions:

Output Requirements:

Respond only with the complete scene graph triplets after adding new triplets.

Do not include any explanations or commentary in your output.

Removing Triplets:

Skip the first triplet, remove any triplets that contain the subject of the first triplet.

Adding Triplets:

Use the subject node of the first triplet as subject, and select at most 4 other nodes as objects, and one of the possible relationships, form at most one triplet for each of the selected object, and add to the list.

Only add triplets that are consistent with the spatial constraints of the existing scene graph.

Do not add triplets that are

already present in the scene graph.

Do not add triplets that are contradictory to the existing scene graph.

Do not add triplets that are redundant.

Spatial Relationships:

Ensure that the updated scene graph has no contradictions in

spatial relationships.

(A contradiction is defined as two or more triplets that imply mutually exclusive spatial configurations.)

Output Format:

Your response should include the



```
entire updated scene graph,
in the exact order specified
by the input plus any new valid triplets.
Do not include any extra text, formatting,
or explanations.
Respond one triplet per line.
```

Example:

Example Input:

```
chair_1 desk_1 right
chair_1 floor_1 standing_on
desk_1 floor_1 standing_on
chair_1 desk_1 left
chair_2 desk_1 right
chair_2 floor_1 standing_on
```

Example Output:

```
desk_1 floor_1 standing_on
chair_2 floor_1 standing_on
chair_1 desk_1 right
chair_1 floor_1 standing_on
chair_1 chair_2 left
[/Context]
```

## D. Statistics of user study

We show that across two tasks, there is a clear trend favoring our method. Our method, combined with the downstream 3D scene generation module, provides a solid framework for 3D scene manipulation.

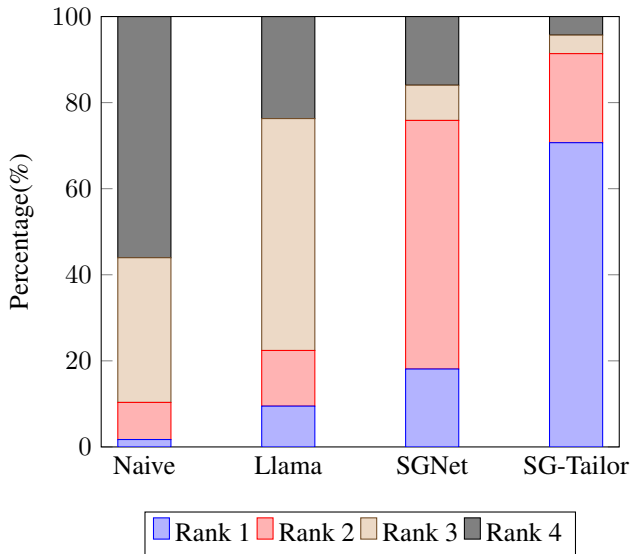


Figure 5. Statistics of the user study in the manipulation task

## E. Additional Robotic Manipulation Results

We show additional performance when combining SG-Bot with Sg-Tailor in Figure 7, further showcasing the conflict-

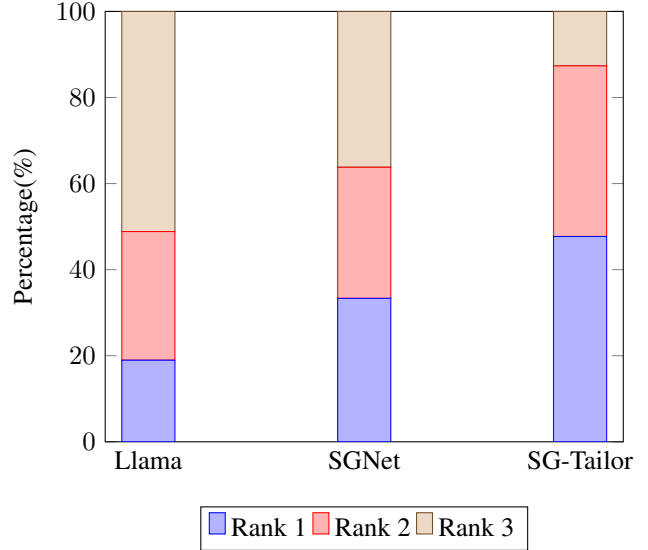


Figure 6. Statistics of the user study in the addition task

resolving ability of SG-Tailor. The above red stream in Figure 7 shows the original SG-Bot is able to pick up the box, but due to the conflicts in the scene graph, the generation model fails, so the target location is still around the starting pose. In contrast, SG-Tailor can help by resolving the conflicts in the scene graph, so the generative model works again, thereby able to rearrange objects (see green stream).

## F. User Study Interface

In this section, we detail the user study conducted to evaluate participants' perceptions of the rendered 3D scene image rankings. The study was structured into two parts, focusing on the node addition and edge change tasks. In each part, participants provided conceptual evaluations of the rankings based on their personal interpretations. To ensure unbiased responses, the images were presented in a completely randomized order with only minimal instructions provided, as shown in Figure 8.

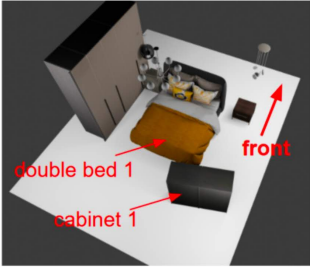


Figure 7. More qualitative comparison of SG-Bot w/ and w/o SG-Tailor.


Manipulation

This section displays four images of indoor scene layouts. Please rank them from **best** to **worst** based on how well they match the provided action description. You are welcome to zoom in for details and interpret the description in your own way.


1. Original Layout




Action: move **cabinet 1** to the **behind** of double bed 1



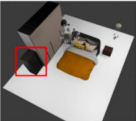
Layout 1



Layout 2



Layout 3



Layout 4

Please rank the four layouts in order of <sup>\*</sup> how well they match the action description, with **1 being the best match** and **4 being the worst**.

	1	2	3	4
Layout 1	<input checked="" type="radio"/>	<input type="radio"/>	<input type="radio"/>	<input type="radio"/>
Layout 2	<input type="radio"/>	<input type="radio"/>	<input type="radio"/>	<input type="radio"/>
Layout 3	<input type="radio"/>	<input type="radio"/>	<input type="radio"/>	<input type="radio"/>
Layout	<input type="radio"/>	<input type="radio"/>	<input type="radio"/>	<input type="radio"/>

Figure 8. User interface for the perceptual user study.